Mon. Not. R. Astron. Soc. **318**, 1273–1276 (2000)

Projected properties of triaxial modified Hubble mass models

D. K. Chakraborty★† and Parijat Thakur
School of Studies in Physics, Pt. Ravishankar Shukla University, Raipur, 492 010, India

Accepted 2000 June 29. Received 20 June 16; in original form 1999 December 23

ABSTRACT

The projected properties of a triaxial generalization of the modified Hubble mass model are investigated. The projected surface density can be evaluated analytically, allowing us to investigate its properties in analytic forms. The profiles of axis ratio and position angle of the major axis of constant density elliptical contours, as a function of viewing angles, can be compared with observations.

Key words: galaxies: photometry – galaxies: structure.

1 INTRODUCTION

A family of mass models, which are triaxial generalisations of the modified Hubble model is studied. The model was first proposed by Schwarzschild (1979) as a numerical model for a triaxial stellar system in dynamical equilibrium. Later it was put into an analytical form by de Zeeuw & Merritt (1983), which was employed by Lees & Schwarzschild (1992) to study the orbital structure of galactic halos. The triaxial density function ρ is obtained by adding two terms, each one of these is a radial function multiplied by a spherical harmonic of low order, to the spherical modified Hubble density.

We project the mass model along a line of sight. The radial functions adopted in the mass model allow us to calculate the projected surface density Σ analytically and thereby, making it possible to investigate some of the projected properties analytically. The method adopted here is close to that of de Zeeuw & Carollo (1996) (hereafter ZC96), who have studied a triaxial generalisation of the γ-model of Dehnen (1993). However the radial functions chosen by these authors do not allow the calculations of Σ analytically in general, and one has to resort to numerical integration.

We studied the constant surface density contours which are approximately elliptical. We calculated the profiles of the surface density Σ, the axis-ratio b/a and the position angles Θ_* of the major axis as functions of radial distance. These can be compared with the photometric data of real galaxies. The analytical expression of the surface density is very useful for the calculation of b/a and Θ_*. In asymptotic regions analytical expressions can be derived, while in intermediate regions simple numerical methods can be adopted for these calculations.

In Section 2 we describe the mass model and in Section 3 we present the projected properties. Section 4 is devoted to results and discussion.

★ E-mail: ircrsu@bom6.vsnl.net.in
† Senior Associate, Inter-University Centre for Astronomy and Astrophysics (IUCAA), Post Bag 4, Ganeshkhind, Pune, 411 007, India.

2 THE MASS MODEL

We consider a density distribution of the form

$$\rho(r,\theta,\phi) = f(r) - g(r)Y_2^0(\theta) + h(r)Y_2^2(\theta,\phi), \tag{1}$$

where (r,θ,ϕ) are the usual spherical coordinates, $Y_2^0(\theta) = \frac{3}{2}\cos^2\theta - \frac{1}{2}$ and $Y_2^2(\theta,\phi) = 3\sin^2\theta\cos 2\phi$ are the usual spherical harmonics, and

$$f(r) = \frac{M}{4\pi}\frac{1}{(b_0^2+r^2)^{3/2}},$$

$$g(r) = \frac{3M}{4\pi}\frac{b_1^3}{b_0^3}\frac{2r^4+7b_2^2r^2}{(b_2^2+r^2)^{7/2}},$$

$$h(r) = \frac{3M}{4\pi}\frac{b_3^3}{b_0^3}\frac{2r^4+7b_4^2r^2}{(b_4^2+r^2)^{7/2}}, \tag{2}$$

where M is the total mass of the model, b_0 the scale length, and b_1, b_2, b_3, b_4 are constants. The four ratios $(b_1/b_0),\ldots,(b_4/b_0)$ can be expressed in terms of the axis ratios of the density distribution at large and small radii, where the constant ρ surfaces are approximately ellipsoidal, i.e. $\rho \sim \rho(m^2)$ with $m^2 = x^2 + (y^2/p^2) + (z^2/q^2)$. Prescribing the values of the axis ratios of constant ρ surfaces at very large and very small radii as (p_∞, q_∞) and (p_0, q_0), respectively, we find that

$$\left(\frac{b_1}{b_0}\right)^3 = \frac{1+p_\infty^3-2q_\infty^3}{6(1+p_\infty^3+q_\infty^3)},$$

$$\left(\frac{b_3}{b_0}\right)^3 = \frac{1-p_\infty^3}{12(1+p_\infty^3+q_\infty^3)},$$

$$\left(\frac{b_1}{b_2}\right)^3\left(\frac{b_0}{b_2}\right)^2 = \frac{p_0^2(1-q_0^2)+p_0^2-q_0^2}{14(p_0^2+q_0^2+p_0^2q_0^2)},$$

$$\left(\frac{b_3}{b_4}\right)^3\left(\frac{b_0}{b_4}\right)^2 = \frac{q_0^2(1-p_0^2)}{28(p_0^2+q_0^2+p_0^2q_0^2)}. \tag{3}$$

3 PROJECTED PROPERTIES

We project the density by choosing standard spherical coordinates (θ', ϕ') of the line of sight (de Zeeuw & Franx 1989) and defining (R, Θ) as the polar coordinates in a plane, perpendicular to the line of sight. The projected surface density is given by

$$\Sigma(R,\Theta) = \Sigma_0(R) + \Sigma_2(R)\cos 2(\Theta - \Theta_*), \tag{4}$$

where

$$\Sigma_0(R) = 2F_1 + (1 - 3\cos^2\theta')\left[G_1 - \tfrac{3}{2}G_2\right] + (6H_1 - 9H_2)\sin^2\theta'\cos 2\phi', \tag{5}$$

$$\Sigma_2^2(R) = [6H_2\cos\theta'\sin 2\phi']^2 + \left[\tfrac{3}{2}G_2\sin^2\theta' - 3H_2(1+\cos^2\theta')\cos 2\phi'\right]^2. \tag{6}$$

We have defined the integrals

$$G_1(R) = \int_R^\infty \frac{rg(r)\,\mathrm{d}r}{\sqrt{(r^2 - R^2)}},$$

$$G_2(R) = R^2\int_R^\infty \frac{g(r)\,\mathrm{d}r}{r\sqrt{(r^2 - R^2)}}, \tag{7}$$

and similarly for F_1, H_1 and H_2 in terms of functions $f(r)$ and $h(r)$ respectively.

The projected surface density (4) has its major axis at position angle Θ_*, given by

$$\tan 2\Theta_* = \frac{Th_3}{h_1 + (1-T)h_2}, \tag{8}$$

where

$$h_1 = \sin^2\phi' - \cos^2\phi'\cos^2\theta',$$

$$h_2 = \cos^2\phi' - \sin^2\phi'\cos^2\theta',$$

$$h_3 = \sin 2\phi'\cos\theta', \tag{9}$$

and $T \equiv T(R)$ is the triaxiality parameter, given by

$$T = \frac{4H_2(R)}{G_2(R) + 2H_2(R)}. \tag{10}$$

Equations (4)–(10) were derived by ZC96, which are reproduced here for easy reference. However, unlike the case investigated by ZC96, here it is possible to calculate the integrals (7) analytically. We found

$$F_1(R) = \frac{M}{4\pi b_0^3}\frac{b_0^3}{b_0^2 + R^2},$$

$$G_1(R) = \frac{M}{4\pi b_0^3}\frac{2b_1^3}{(b_2^2 + R^2)^3}[2b_2^4 + 9b_2^2R^2 + 3R^4],$$

$$G_2(R) = \frac{M}{4\pi b_0^3}\frac{4b_1^3}{(b_2^2 + R^2)^3}R^2[3b_2^2 + R^2], \tag{11}$$

and similarly for $H_1(R)$ and $H_2(R)$ in terms of b_3 and b_4, in place of b_1 and b_2, respectively.

Equation (8) allows us to calculate the position angle Θ_*. It gives the position angle of the major axis if

$$H_2h_3\sin 2\Theta_* < 0. \tag{12}$$

The axis ratio b/a can be calculated by using

$$\Sigma_0(a) + \Sigma_2(a) = \Sigma_0(b) - \Sigma_2(b). \tag{13}$$

3.1 Asymptotic values

The analytic expressions (11) allow one to write G_2/H_2 and, therefore, T and Θ_* analytically. In particular, at large R, the ratio $(G_2/H_2)_\infty$ and the triaxiality parameter T_∞ are given by

$$\left(\frac{G_2}{H_2}\right)_\infty = \frac{b_1^3}{b_3^3} \tag{14}$$

and

$$T_\infty = \frac{4b_3^3}{b_1^3 + 2b_3^3} = \frac{1 - p_\infty^3}{1 - q_\infty^3}. \tag{15}$$

The latter form of T_∞ matches with the expression of ZC96 [cf. equation (3.8)]. Note that at large r de Zeeuw and Carollo's ρ goes as $1/r^4$, whereas ρ of equation (1) in our study goes as $1/r^3$. Using (15) in (8), one can calculate the position angle Θ_* at large R.

Likewise, at small R, the ratio $(G_2/H_2)_0$ and the triaxiality T_0 are

$$\left(\frac{G_2}{H_2}\right)_0 = \frac{b_1^3}{b_3^3}\frac{b_4^4}{b_2^4} \tag{16}$$

and

$$T_0 = \frac{4b_3^3b_2^4}{b_1^3b_4^4 + 2b_3^3b_2^4}. \tag{17}$$

This expression of T_0 has a complicated form in terms of p_0, q_0, p_∞, q_∞, as compared to (3.8) of ZC96. While the model of ZC96 is a cuspy model, the model discussed here has a core at the centre, and the projected properties at the centre depend on the light at all radii.

Further, defining a few more functions,

$$h_4 = (6h_3)^2 + 9(h_1 - h_2)^2,$$

$$h_5 = \tfrac{9}{4}(h_1 + h_2)^2,$$

$$h_6 = 9(h_1^2 - h_2^2),$$

$$h_7 = 1 - 3\cos^2\theta',$$

$$h_8 = \sin^2\theta'\cos 2\phi', \tag{18}$$

of the viewing angles θ' and ϕ' and defining

$$Z \equiv \left[h_4 + h_5\left(\frac{G_2}{H_2}\right)^2 + h_6\left(\frac{G_2}{H_2}\right)\right]^{1/2} \tag{19}$$

and

$$A = \frac{2}{b_0} + \frac{12b_1^3h_7}{b_2^4} + \frac{72b_3^3h_8}{b_4^4}, \tag{20}$$

we find that

$$\left(\frac{b}{a}\right)_\infty^2 = \frac{b_0^3 - 2b_3^3Z_\infty}{b_0^3 + 2b_3^3Z_\infty} \tag{21}$$

and

$$\left(\frac{b}{a}\right)_0^2 = \frac{A - (12b_3^3/b_4^4)Z_0}{A + (12b_3^3/b_4^4)Z_0}, \tag{22}$$

where Z_∞ and Z_0 are the values of Z at very large and very small radii, respectively. The values of G_2/H_2 at large and small distances, required to evaluate Z_∞ and Z_0 are given by (14) and

(16). We have used definition (13) to evaluate (21) and (22), which give the axis ratio, respectively, at very large and very small radii.

In Appendix A, we present some more analytical derivations of the projected properties.

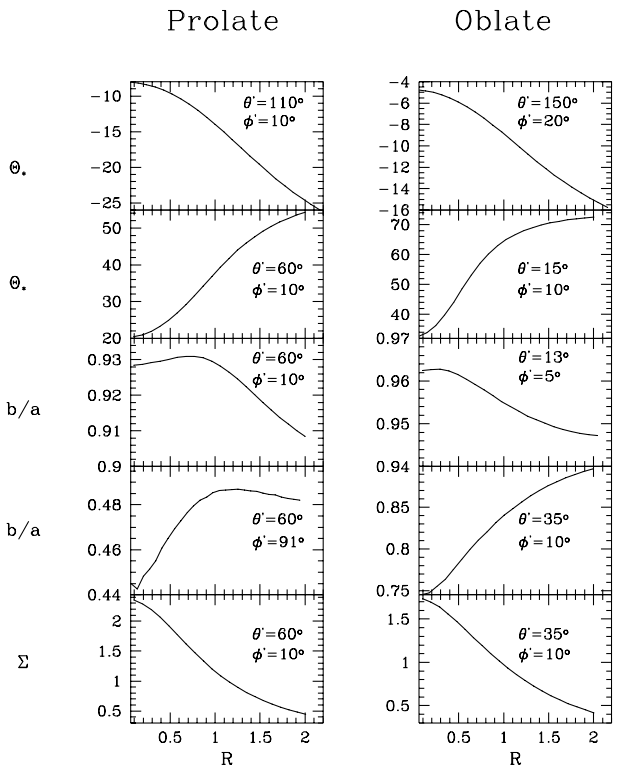

Figure 1. Profiles of Θ_*, b/a and Σ as functions of R. Θ_* are in degrees while $R = \sqrt{ab}$ and Σ are in the units of b_0 and $M/4\pi b_0^2$ respectively. The viewing angles (θ', ϕ') of each frame are mentioned therein. The parameters (p, q) for the frames in first four rows are (0.65, 0.55) for prolate and (0.95, 0.55) for oblate, and the parameters $(p_0, q_0, p_\infty, q_\infty)$ for the last row are (0.75, 0.65, 0.65, 0.55) for prolate and (0.95,0.75, 0.95, 0.55) for oblate.

4 RESULTS AND DISCUSSION

The mass model presented in (1) is a triaxial generalisation of the modified Hubble model. It has a core at the centre. The projected surface density can be calculated analytically. The approximate elliptical isodensity contours show the variation in b/a and Θ_* with R. Thus our model seems most useful as a simple analytical example of a model with ellipticity variations and isophote twists.

Fig. 1 shows the variations of Σ, b/a and Θ_* with R for various choices of the intrinsic parameters and the viewing angles. Σ decreases as $1/R^2$ at large R for all choices of the parameters. Choosing $p_0 = p_\infty \equiv p$ and $q_0 = q_\infty \equiv q$, we find that the position angle Θ_* increases when h_3 is positive and decreases when h_3 is negative. The variation of b/a with R is interesting. Between a very small and very large R, b/a decreases for a range R_1 of the viewing angles and increases for another range R_2 of the viewing angles for prolates ($p \simeq q$). These ranges of viewing angles are depicted in Fig. 2. For oblates ($p \simeq 1$), on the other hand, b/a increases for almost all viewing angles. The above nature of variations of Θ_* and b/a are maintained as long as the choices $p_0 \simeq p_\infty$ and $q_0 \simeq q_\infty$ are adopted.

ACKNOWLEDGMENTS

We are thankful to CSIR, New Delhi, India, for providing financial support through the project grant no. 03(0807)/97/EMR-II. DKC, Senior Research Associate of the IUCAA, Pune, India, and PT express their sincere thanks to IUCAA for providing local hospitality and support during IUCAA visits.

REFERENCES

Dehnen W., 1993, MNRAS, 265, 250
de Zeeuw P. T., Carollo C. M., 1996, MNRAS, 281, 1333
de Zeeuw P. T., Franx M., 1989, ApJ, 343, 617
de Zeeuw T., Merritt D., 1983, ApJ, 267, 571
Lees J. F., Schwarzschild M., 1992, ApJ, 384, 491
Schwarzschild M., 1979, ApJ, 232, 236

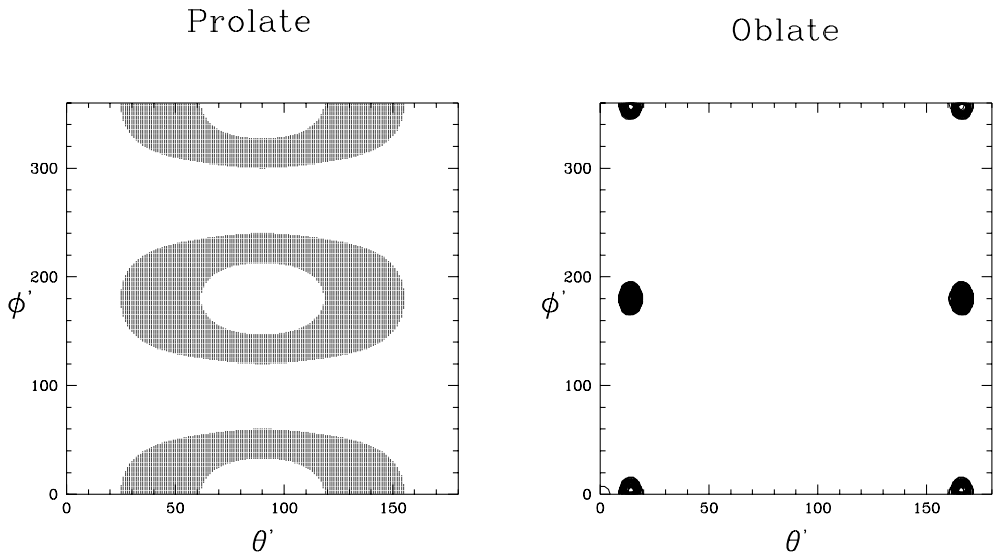

Figure 2. Range R_1, in black (R_2, in white), of viewing angles for decreasing (increasing) b/a.

APPENDIX A

At large R, the surface density Σ goes as $1/R^2$, and writing $(\Theta - \Theta_*)$ as θ, equation (4) can be written as

$$\Sigma(R, \theta) = \frac{P}{R^2} + \frac{\mathrm{Q}}{R^2}\cos^2\theta, \tag{A1}$$

where

$$P = \frac{2M}{4\pi b_0^3}(b_0^3 - 2b_3^3 Z_\infty),$$

$$Q = \frac{2M}{4\pi b_0^3} 4b_3^3 Z_\infty. \tag{A2}$$

As $Q \ll P$, (A1) can be written as

$$\frac{P}{\Sigma R^2} = 1 - \frac{Q}{P}\cos^2\theta + \left(\frac{Q}{P}\right)^2 \cos^4\theta + \cdots, \tag{A3}$$

which, again, can be recasted in the form

$$\frac{P}{\Sigma R^2}\left(1 + \frac{Q^2}{8P^2}\right) = 1 - \frac{Q}{P}\left(1 - \frac{Q}{P}\right)\cos^2\theta + \frac{1}{8}\left(\frac{Q}{P}\right)^2 \cos 4\theta, \tag{A4}$$

retaining terms up to $(Q/P)^2$ only. Comparing (A4) with the equation of an ellipse

$$\frac{b^2}{R^2} = 1 - \epsilon^2 \cos^2\theta, \tag{A5}$$

where b is the semilatus rectum and ϵ the eccentricity; we find that a constant Σ-contour is approximately elliptical with

$$\epsilon^2 = \frac{Q}{P}\left(1 - \frac{Q}{P}\right). \tag{A6}$$

The plot of (A4) shows that constant Σ contours are slightly boxy. The numerical evaluation of (A6) agrees closely with the values, as obtained by using (21).

At small R, Σ goes as R^2 and the equation of approximate elliptical constant Σ contours can also be written.

This paper has been typeset from a TEX/LATEX file prepared by the author.